A&A 422, 239–245 (2004)
DOI: 10.1051/0004-6361:20035693

Astronomy & Astrophysics

The role of the time step and overshooting in the modelling of PMS evolution: The case of EK Cephei

J. P. Marques[1,2], J. Fernandes[2,3], and M. J. P. F. G. Monteiro[1,4]

[1] Centro de Astrofísica da Universidade do Porto, Rua das Estrelas, 4150-762 Porto, Portugal
[2] Grupo de Astrofísica da Universidade de Coimbra, Observatório Astronómico da Universidade de Coimbra, Santa Clara, Coimbra, Portugal
[3] Departamento de Matemática da FCTUC, Coimbra, Portugal
[4] Departamento de Matemática Aplicada, Faculdade de Ciências da Universidade do Porto, Portugal

Received 14 November 2003 / Accepted 6 April 2004

Abstract. EK Cephei (HD 206821) is a unique candidate to test predictions based on stellar evolutionary models. It is a double-lined detached eclipsing binary system with accurate absolute dimensions available and a precise determination of the metallicity. Most importantly for our work, its low mass (1.12 $M_{\odot}$) component appears to be in the pre-main sequence (PMS) phase.

We have produced detailed evolutionary models of the binary EK Cep using the CESAM stellar evolution code (Morel 1997). A χ^2-minimisation was performed to derive the most reliable set of modelling parameters (age, $\alpha_{\rm A}$, $\alpha_{\rm B}$ and $Y_{\rm i}$). We have found that an evolutionary age of about 26.8 Myr fits both components in the same isochrone. The positions of EK Cep A and B in the HR diagram are consistent (within the observational uncertainties) with our results.

Our revised calibration shows clearly that EK Cep A is in the beginning of the main sequence, while EK Cep B is indeed a PMS star. Such a combination allows for a precise age determination of the binary, and provides a strict test of the modelling. In particular we have found that the definition of the time step in calculating the PMS evolution is crucial to reproduce the observations. A discussion of the optimal time step for calculating PMS evolution is presented.

The fitting to the radii of both components is a more difficult task; although we managed to do it for EK Cep B, EK Cep A has a lower radius than our best models.

We further studied the effect of the inclusion of a moderate convective overshooting; the calibration of the binary is not significantly altered, but the effect of the inclusion of overshooting can be dramatic in the approach to the main sequence of stars with masses high enough to burn hydrogen through the CNO cycle on the main sequence.

Key words. stars: pre-main sequence – stars: evolution – stars: fundamental parameters – stars: individual: EK Cephei

1. Introduction

It is very well known that the interior structure of an evolved star is fixed by the initial mass $M_{\star}$, the initial chemical composition (initial abundances in hydrogen, helium and metals, $X_{\rm i}$, $Y_{\rm i}$ and $Z_{\rm i}$, respectively) and the age $t_{\star}$. So, except for the Sun, modelling a single star using stellar evolutionary models on the HR diagram is not a closed problem because the number of parameters to be determined is larger than the observational constraints, the present observed luminosity and effective temperature.

This difficulty is increased due to uncertainties on the physics of the models used to describe the stellar interior/external structure. Currently these uncertainties are modelled by free parameters such as the diffusive and mass loss coefficient or the mixing length and overshooting parameters for the convection in the MLT approximation (Mixing Length Theory).

Some stellar multiple systems are in excellent position to avoid these difficulties. Good determinations of stellar masses are possible for the components of a given binary. Based on the reasonable assumption of a common origin for both components (which yields the same initial chemical composition and age), the problem of modelling both stars of a binary system is reduced to the determination of three so-called stellar modelling parameters, namely, $Y_{\rm i}$, $Z_{\rm i}$, $t_{\star}$ (since $X+Y+Z=1$ we do not need to determine $X_{\rm i}$ independently). Moreover, if the stars are young enough (so that diffusion processes have not had time to change the surface composition significantly) and the present surface metallicity of the stars is also known (and is, therefore, equal to the initial metallicity), then $(Z/X)_{\rm i}$ is known. So, the number of observables (five: the effective temperatures and

Send offprint requests to: J. P. Marques,
e-mail: jmarques@astro.up.pt

Table 1. Properties of EK Cep (HD 206821). All data except chemical composition are from Andersen (1991) and Popper (1987); chemical compositions are from Martín & Rebolo (1993). See also Tomkin (1983), Ebbighausen (1966), and Hill & Ebbighausen (1984).

	EK Cep A	EK Cep B
$M_\star/M_\odot$	2.029 ± 0.023	1.124 ± 0.012
$\log T_{\rm eff,\star}$ (K)	3.954 ± 0.010	3.756 ± 0.015
$\log (L_\star/L_\odot)$	1.17 ± 0.04	0.21 ± 0.06
$R_\star/R_\odot$	1.579 ± 0.007	1.315 ± 0.006
$\log g$ (cgs)	4.349 ± 0.010	4.251 ± 0.006
Sp. type	A1.5V	G5Vp
[Fe/H]	...	$+0.07 \pm 0.05$

luminosities for both stars plus the metallicity of the system) is higher than the number of modelling parameters. This allows us to include unknown parameters related to the description of the interior physics. For low mass stars, without mass-loss or strong rotation, the convection is the main source of uncertainties in the description of the stellar interior. So we choose to include the mixing length parameter for each component of a binary system $\alpha_{\rm A}$ and $\alpha_{\rm B}$. A number of binary systems have been calibrated in this way, e.g. α Cen (Noels et al. 1991; Morel et al. 2000b) and ι Peg (Morel et al. 2000a); all these stars are, however, main sequence (MS) or post-main sequence stars.

A good candidate binary system for calibration must have well-determined luminosities, effective temperatures, metallicities and dynamical masses. Pre-main sequence (PMS) binaries that have all the required characteristics are very rare at present (see Palla & Stahler 2001, for some examples of PMS binaries, and Lee et al. 1994, for lithium abundances for some of them).

The double-lined eclipsing binary system EK Cep (HD 206821) has these unique characteristics. Accurate absolute dimensions are available (Andersen 1991; Popper 1987) and a determination of the surface metallicity was made (Martín & Rebolo 1993). Most importantly, the radii of the two stars are much closer than expected given their mass ratio. This indicates that EK Cep B is still contracting towards the main-sequence. At the same time, the higher mass of the primary implies that the star must be already in its main sequence evolution. All these make EK Cep a perfect candidate to test theoretical models of pre-ZAMS solar-type stars. A summary of the observational characteristics of this binary is given in Table 1.

Several authors have tried to model this system. A problem frequently found is that EK Cep A has a smaller radius (or that EK Cep B has a bigger radius) than that predicted by the models, making it difficult to fit both components to the observations in the same isochrone. Claret et al. (1995) have computed models that agree reasonably well with the observations; however, the radius of EK Cep B is somewhat higher than their models predict (a problem also found in the models used for comparison with the observations in Martín & Rebolo 1993). Yıldız (2003) computed models using a higher metallicity than Claret et al. and a fast rotating core for EK Cep A in order to lower its luminosity and radius; this way, models that fit the observed radii and luminosities of the EK Cep system can be computed. The metallicity used in Yıldız (2003; $Z \sim 0.04$) is much higher, however, than that given in Martín & Rebolo (1993; $Z \sim 0.02$). The values for the iron abundance given by these authors spread somewhat, making a very precise determination of this abundance difficult; nothing in these values comes close, however, to the value of metallicity used in Yıldız (2003).

Our atempt to model this system focuses, instead, on the physical input that might affect the PMS evolution. Our own PMS models, computed using the CESAM stellar evolution code (Morel 1997), suggested that there are effects in the PMS evolution due to the physical inputs (overshooting, time step) that have been ignored or too quickly dismissed in the previous works.

2. Physical ingredients

Models were computed using the CESAM stellar evolution code (Morel 1997). Typically, each model is described by about 600 shells, and an evolution by about 400–600 models. We restricted the maximum time step of the evolution: for EK Cep A, the maximum time step was kept at about 0.017 Myr, while for EK Cep B we allowed the time step to reach 0.075 Myr. We justify these values for the time step in Sect. 6.

Each evolution is initialised with an homogeneous, fully convective model in quasi-static contraction (Iben 1965), with a central temperature inferior to the ignition temperature of the deuterium. We shall call the "age" of the model the time elapsed since initialisation. This initial model for PMS evolution is not a realistic assumption, since stars do not form by the homologous contraction of the pre-stellar cloud. Instead, a hydrostatic core first forms, which accretes mass from the parental cloud until either stellar winds disperse the cloud or the cloud material exhausts. Then the star becomes optically visible for the first time, since no more surrounding material obscures it: the star is born (see Stahler 1983; Palla & Stahler 1991, 1992). If we wanted to model very young stars, the problem of the initial conditions would be very important; for EK Cep, however, the initial conditions are irrelevant since it is much older than 1 Myr. Our "age" of the model, although not a real age of the star, is very close to it.

The model of the zero-age main-sequence (ZAMS) is defined as the first model where nuclear reactions account for more than 99% of the energy generation.

We used the OPAL equation of state (Rogers et al. 1996; we used the 2001 version of the OPAL tables which goes down to 2000 K) and the opacities of Iglesias & Rogers (1996), complemented, at low temperatures, by the Alexander & Fergusson (1994) opacities.

The temperature gradient in convection zones is computed using the standard mixing-length theory (Böhm-Vitense 1958). The mixing length is defined as $l = \alpha_\star H_P$, H_P being the local pressure scale height, $H_P = -{\rm d}r/{\rm d}\ln P$.

The nuclear network we use contains the following species: ^{1}H, ^{2}H, ^{3}He, ^{4}He, ^{7}Li, ^{7}Be, ^{12}C, ^{13}C, ^{14}N, ^{15}N, ^{16}O, ^{17}O, ^{9}Be, and an "extra" fictitious non-CNO heavy element which complements the mixture; this element has atomic mass 28 and charge 13. Deuterium and lithium burning are taken

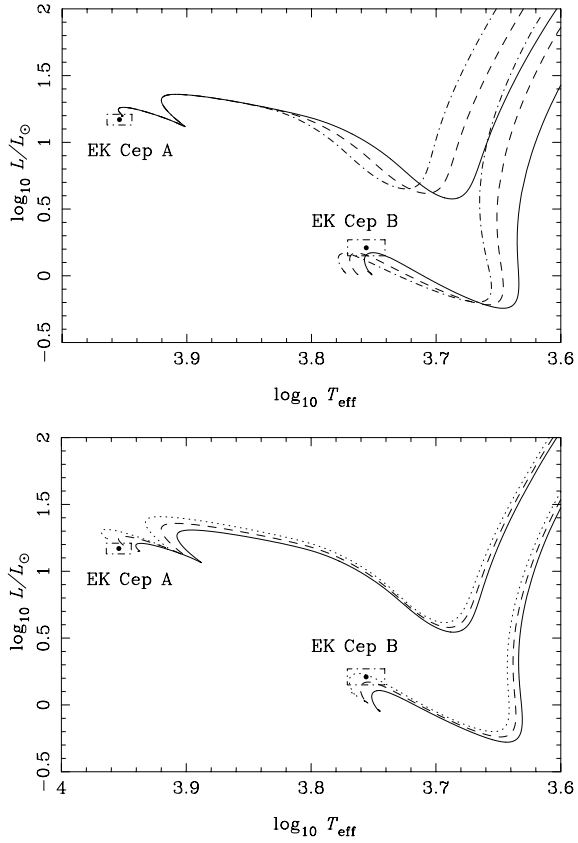

Fig. 1. *Upper panel*: variation of the evolutionary tracks with the mixing length parameter α. Full lines are evolutionary tracks for $\alpha = 1.3$; dashed lines are for $\alpha = 1.6$; and dotted lines are for $\alpha = 1.9$. *Lower panel*: variation of the evolutionary tracks with the initial helium abundance. Full lines are evolutionary tracks for $Y = 0.24$; dashed lines are for $Y = 0.26$; and dotted lines are for $Y = 0.28$.

into account, as well as the most important reactions of the PP+CNO cycles. The nuclear reaction rates are taken from the NACRE compilation (Angulo et al. 1999).

Given the expected young age of the binary, we do not consider diffusion processes. However, these effects must be taken into account if we would follow the evolution of the surface chemical composition. If the surface chemical composition were known with high accuracy for both components, the binary would be an excellent candidate to test diffusion in the models.

3. The fitting method

The calibration of a binary system consists of adjusting the stellar modelling parameters so that the models reproduce the observational data of the stars. The effective temperature and luminosity of a model, for a given mass and fixed input physics (EOS, opacity, nuclear energy generation rates), depend on the modelling parameters: the age $t_\star$, initial helium abundance $Y_{\rm i}$ and mixing length parameter $\alpha_\star$.

The effect that the variation of the initial helium abundance $Y_{\rm i}$ and mixing length parameter $\alpha_\star$ has on the evolutionary tracks can be seen in Fig. 1. An increase in $\alpha_\star$ moves

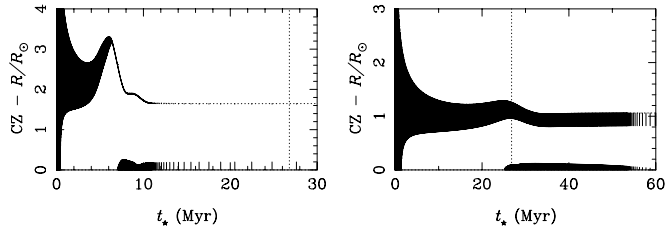

Fig. 2. Convective zones and radii of EK Cep A (*left panel*) and B (*right panel*). Vertical lines represent the extent of convective zones; the vertical dotted line in both panels represents the best model, with an age of 26.8 Myr.

the evolutionary tracks in the HR diagram towards larger effective temperatures at approximately constant luminosity, for stars with convective envelopes. An increase of the efficiency of the convection deepens the base of the convective envelope, while it does not affect the core. The temperature of the base of the external convective zone therefore increases, and the adjustment of the adiabat to a higher temperature at its base causes the effective temperature to increase, leaving the luminosity almost unchanged.

Figure 2 shows the evolution of the convective zones of EK Cep A and B. The convective envelope of EK Cep A disappears as the star approaches the main sequence, hence the small effect of the variation of $\alpha_\star$ in the tracks of EK Cep A on the later phases of PMS evolution.

A larger helium abundance shifts the evolutionary tracks on the HR diagram towards higher effective temperature and higher luminosity (see lower panel of Fig. 1). That is because a larger helium abundance causes the mean molecular weight to increase, which decreases the pressure. To maintain quasi-static equilibrium, the temperature must increase, which causes an increase in the energy generation rate and, thus, an increase in luminosity. This increase is more obvious in main sequence stars because of the large power-law dependence of the nuclear reaction rates on temperature. On the other hand, the gravitational energy generation rate increases only linearly with temperature and the rise in luminosity due to the larger helium abundance is smaller for PMS stars.

We can, then, produce a stellar model with a higher effective temperature by increasing the parameter $\alpha_\star$; to change only the luminosity of the model, we can change simultaneously $Y_{\rm i}$ and $\alpha_\star$. To obtain observables as close as possible to the observations, we use the χ^2 fitting developed by Lastennet et al. (1999; see also Morel et al. 2000b). It corresponds to minimising the following functional:

$$\chi^2 = \sum_{\star=A,B} \left\{ \left[\frac{\log T_{\rm eff,\star}^{\rm mod} - \log T_{\rm eff,\star}}{\sigma(\log T_{\rm eff,\star})} \right]^2 + \left[\frac{\log L_\star^{\rm mod} - \log L_\star}{\sigma(\log L_\star)} \right]^2 \right\} . \quad (1)$$

This functional depends on the modelling parameters through $\log T_{\rm eff,\star}^{\rm mod}$ and $\log L_\star^{\rm mod}$. For a grid of modelling parameters we have computed the evolution of models with the masses and metallicities of EK Cep A and B. The functional χ^2 was computed for each of these models using the above equation. The parameters that minimised χ^2 were selected as the solution.

Table 2. Modelling parameters for a model of EK Cep lying within the uncertainty boxes for $\log T_{\rm eff,\star}$ and $\log L_\star/L_\odot$ (see text). The parameters for the Sun are for a calibrated solar model using the same input physics. We do not present the value for $\alpha_{\rm A}$ because there is little dependence of the location of the model of EK Cep A on this parameter (see Fig. 1).

	EK Cep	Sun
$\alpha_{\rm B}$	$1.363^{+0.307}_{-0.173}$	1.632
$Y_{\rm i}$	$0.261^{+0.005}_{-0.006}$	0.265
$t_\star$	$26.8^{+1.6}_{-1.9}$ Myr	4.52 Gyrs

4. Results

The modelling parameters that minimise χ^2 are given in Table 2, together with the same parameters for a calibrated solar model using the same input physics. The uncertainties are derived by changing one parameter at a time around the calibrated value, keeping all the others constant. The value for $\alpha_{\rm A}$ is not listed in Table 2, since the dependence of the evolutionary tracks on this parameter is very weak (see Sect. 3, and in particular Fig. 1). We used $\alpha_{\rm A} = 1.340$ to produce these models.

Our calibrated value of $\alpha_{\rm B}$ is lower than the value of $\alpha_\star$ for calibrated models of solar-mass stars (see, for example, Morel et al. 2000b for the case of α Cen, as well as the value for the solar case we present in Table 2). Typically, one has $\alpha_\star \sim 1.6$–1.8 for calibrated solar-type stars. D'Antona & Montalbán (2003) argue that in order to reproduce both the lithium depletion and the location of PMS tracks in the HR diagram, convection must be highly inefficient during the PMS; that is, it must have a very low $\alpha_\star \sim 1$. Our value of $\alpha_{\rm B}$ is between that appropriate for a calibrated MS model and the value argued by D'Antona & Montalbán for PMS models when they are depleting their lithium. This could reflect the fact that EK Cep B is in an evolutionary phase between the main lithium depletion phase (which occurs for stars with this mass around the time a radiative core starts to develop) and the ZAMS.

The sequences of models for the evolution determined with the best set of parameters are shown in Figs. 2 and 3. Both components of EK Cep have a convective core; EK Cep A is a main sequence star with an energy production mostly due to the CNO cycle, while EK Cep B has just acquired a convective core due to the start of ^{12}C burning.

This convective core in EK Cep B will be lost shortly after the arrival on the ZAMS. The ZAMS occurs at an evolutionary age of $t_{\rm zams,A} = 10.8$ Myr and $t_{\rm zams,B} = 51.3$ Myr for EK Cep A and B, respectively.

From our estimated age of around 27 Myr, follows that EK Cep A is already in the main-sequence, while EK Cep B is indeed a PMS star (see Figs 2 and 3). The fact that both components are in different stages of evolution allows for a precise age determination, as the solution minimising Eq. (1) is strongly dependent on $t_\star$.

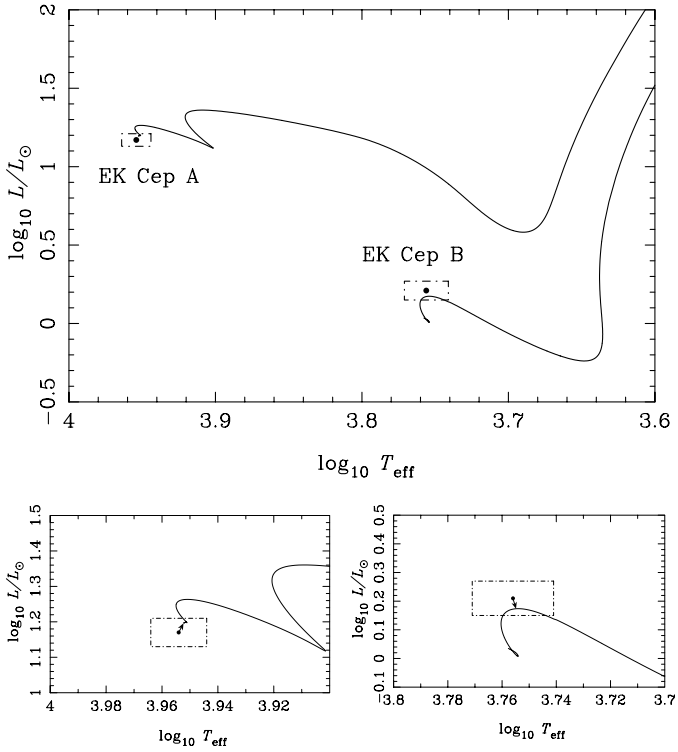

Fig. 3. Evolutionary tracks of EK Cep A and B on the HR diagram. The uncertainty boxes of both stars are also shown. In the lower left panel, an enlargement of the locus of EK Cep A is shown; the arrow shows the location on the HR diagram of the calibrated model.

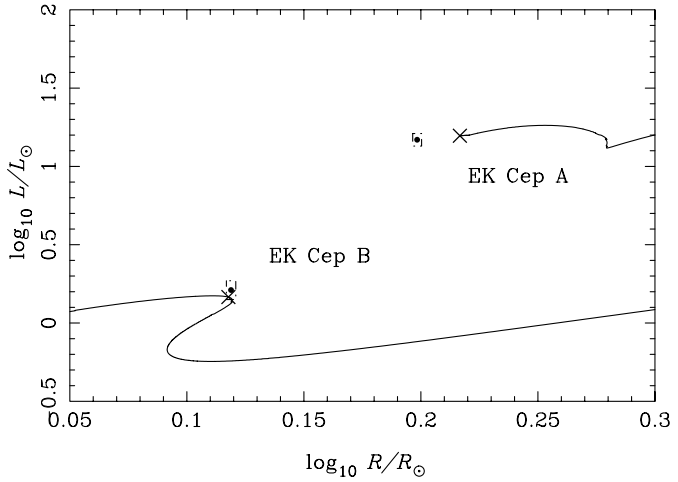

Fig. 4. Evolutionary tracks of EK Cep A and B on the $\log R/R_\odot$–$\log L/L_\odot$ plane. These tracks were calculated using $\alpha_{\rm B} = 1.28$. Crosses show the location of models with 26 Myr.

5. The problem of the radius

Our best models for EK Cep A and B do not fit, however, the observed radii. Since EK Cep is an eclipsing binary, the radii of both stars are known with great precision; the fact that these models do not fit the radii is, therefore, a serious problem.

We can fit the radius of EK Cep B to the observations using a lower $\alpha_{\rm B}$ in the models. Fig. 4 shows the evolutionary tracks for EK Cep A and B on the $\log R/R_\odot$–$\log L/L_\odot$ plane, using $\alpha_{\rm B} = 1.28$ (all other parameters being the same as in

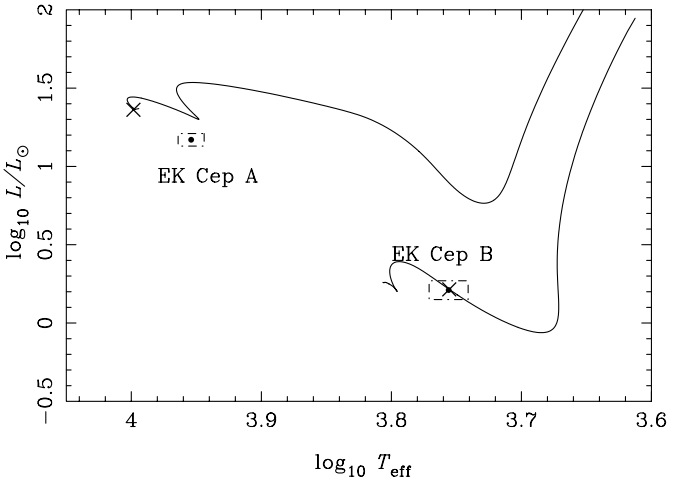

Fig. 5. Evolutionary tracks of EK Cep A and B on the HR diagram. These tracks were calculated using $Y_i = 0.331$ and $\alpha_B = 1.68$, and represent the best fit to the radii of both stars. Crosses show the location of models with 13.9 Myr.

the previous section). However, the same cannot be done for EK Cep A since the model depends weakly on the mixing length parameter α.

We performed the fitting decribed in Sect. 3 using the effective temperature and radius as the observables. The parameters that minimise χ^2 are now $Y_i = 0.331$, $t_\star = 13.9$ Myr and $\alpha_B = 1.68$. The helium abundance seems very large for the metallicity of EK Cep, but it reproduces the results presented in Lastennet et al. (2003) for the binary UV Psc. However, a model of EK Cep A constructed using these parameters still has too large a radius.

Figure 5 shows the evolutionary tracks in the HR diagram of models of both components calculated using the parameters given in the previous paragraph. Since these new parameters fail to improve considerably the fitting to the radius of EK Cep A, while the location in the HR diagram of the model of this star falls well outside the error boxes, we prefer the solution given in Table 2 except for α_B; to fit the radius of EK Cep B within the observational uncertainties, we choose $\alpha_B = 1.28$. The age that best reproduces the observations is $t_\star = 26$ Myr. The characteristics of the best models, calculated using these parameters, are shown in Table 3.

The fact that models of EK Cep A depend so weakly on the mixing length parameter α corresponds to having, in fact, only three "effective" modelling parameters, Y_i, α_B and $t_\star$. Thus, to fit the observables we need an extra parameter, related to the description of the interior physics affecting mainly the high mass component. This could be the differencial rotation of EK Cep A, as described in Yıldız (2003).

6. The role of the time step

Given the importance of EK Cep B in the age determination, it is fundamental that its evolutionary phase (PMS) is adequately calculated. Consequently, we have performed a detailed analysis on the prescription that should be adopted for defining the integration time step in the PMS evolution of this binary.

Table 3. Characteristics of the best models, with $Y_i = 0.261$, $\alpha_B = 1.28$ and $t_\star = 26$ Myr. T_c and ρ_c are the central densities and temperatures, given in 10^6 K and g cm^{-3}, respectively. R_{co} is the radius of the convective core and R_{ce} the radius of the base of the convective envelope. The same quantities are also given for a calibrated solar model using the same input physics ($L_\odot = 3.846 \times 10^{33}$ ergs s^{-1} and $R_\odot = 6.9599 \times 10^{10}$ cm).

	EK Cep A	EK Cep B	Sun
T_c	21.11	12.81	15.45
ρ_c	73.96	77.13	149
T_{eff}	8974 K	5550 K	5777 K
$L_\star/L_\odot$	15.74	1.465	1.000
$R_\star/R_\odot$	1.644	1.311	1.000
$R_{co}/R_\star$	0.120	0.0536	...
$R_{ce}/R_\star$	0.993	0.751	0.729

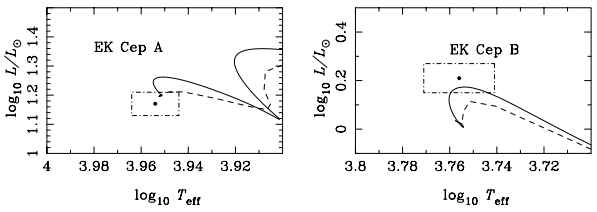

Fig. 6. The role of the time step. *Left panel*: EK Cep A; in full, the evolutionary track with a maximum time step of 0.025 Myr; dashed, the evolutionary track calculated using the time step prescription appropriate for the MS evolution. *Right panel*: the same for EK Cep B. In full, the evolutionary track with a maximum time step of 0.1 Myr.

Figure 6 shows again the evolutionary tracks in the HR diagram for both components of the EK Cep system. The effects of an inappropriate choice of the time step are shown; these effects are only relevant in the PMS phase because in this phase the star derives its energy from gravitational contraction; the rate of gravitational contraction is incorrect if the time step between two consecutive models is too big. The evolutionary tracks represented by a dashed line in Fig. 6 were calculated using a time step prescription that is appropriate for the MS evolution: the time step for the next model is estimated based on the evolution of the chemical composition. That is, the faster the evolution of the chemical composition, the shorter the time step used. This prescription is not useful for models in the PMS phase, since for most of the evolution the chemical composition does not change considerably. Instead, we must use a prescription that does not allow the structure of a star to change too much between consecutive time steps.

We can gauge how much the star has contracted between two consecutive time steps by calculating the gravitational energy generated between them. To do this we must first calculate the model corresponding to $t + \Delta t$. If the gravitational energy generated between the two time steps ($E_g \simeq -T\Delta s$, where s is the specific entropy and T is the temperature) is bigger than a given maximum value, a new model must be calculated corresponding to $t + \Delta t$ for a smaller Δt. There are, however, some numerical difficulties in this approach if the maximum gravitational energy allowed to be generated between two consecutive time steps is too small.

We have chosen a different prescription instead, by using the time the star spends in the PMS phase ($t_{\rm PMS}$). This time is expected to scale, roughly, with the Kelvin-Helmholtz time scale, $t_{\rm PMS} \simeq t_{\rm KH} \simeq GM_\star^2/2R_\star L_\star$, where $R_\star$ and $L_\star$ are the radius and luminosity of the star on the main sequence. These values can be replaced by their ZAMS values since for most of the time the stars are in the radiative part of the PMS evolutionary tracks where $R_\star$ and $L_\star$ do not change very much.

For a given mass range, $R_\star \propto M_\star^\xi$ and $L_\star \propto M_\star^\eta$, on the main sequence. In the mass range of interest here, $\xi \simeq 0.6$ and $\eta \simeq 3.9$ (see Kippenhahn & Weigert 1991, Ch. 22), it follows that

$$t_{\rm PMS} \propto \frac{M_\star^2}{R_\star L_\star} \propto M_\star^{2-\xi-\eta} \simeq M_\star^{-2.5}. \quad (2)$$

We scale the maximum time step allowed with the time the star spends in the PMS phase, so that the evolutionary tracks in the PMS phase are equally divided. For a 1 $M_\odot$ star, we have considered different values for the maximum time step; for values shorter than about 0.1 Myr, the evolution of the star does not change for different values of the time step. Accordingly, the maximum time step we allow in the evolution during the PMS phase is considered to be given by

$$\Delta t_{\rm max} = 0.1 \left(\frac{M_\star}{M_\odot}\right)^{-2.5} {\rm Myr}\,, \quad (3)$$

(see also Kippenhahn & Weigert 1991, Ch. 28).

The effects of different prescriptions for the time step on the calibration of EK Cep can be seen in Fig. 6. The locus of the calibrated model of EK Cep A (left panel) in the HR diagram does not change if we do not control the time step carefully because the star derives most of its energy from nuclear reactions. On the other hand, the locus of the calibrated model of EK Cep B changes considerably; the luminosity of the model calculated without the restriction on the time step is appreciably lower. In fact, we can not fit the observations within their error boxes for both stars if we do not restrict the time step in this way; the luminosity (and radius) of the low mass component is too low. This partially explains the results cited in Martín & Rebolo (1993), that the luminosity of EK Cep B was slightly higher than predicted by pre-main-sequence models. The radius of our model of EK Cep B (with a large time step) is below the error box in radius, a result also obtained by Claret et al. (1995).

The evolution of the models is faster if we do not restrict the time step. Consequently, instead of the value we found (26.8 Myr) the calibrated models of EK Cep would just have an age of ≃23 Myr when using the same prescription as for the MS evolution.

7. The effect of overshooting

We also calculated evolutionary models including the effects of convective overshooting. Convective overshooting is due to the inertia of the convective elements; since they have a non-zero velocity when they reach the border of the convective zone, as given by the instability criteria, they overshoot it. When they reach a radiative zone, they become colder than the surrounding material (since in a radiative zone $\nabla < \nabla_{\rm ad}$) and are therefore heated by their surroundings: they transport energy downwards. To transport all the energy upwards, the energy transported by the radiation must be greater than the total luminosity, that is, $\nabla > \nabla_{\rm rad}$. The effect of the overshooting is, then, to fix the temperature gradient equal to the adiabatic gradient and to extend the mixed zone by a certain amount. We used the following prescription for the extent $d_{\rm ov}$ of the overshooting in the core,

$$d_{\rm ov} = \alpha_{\rm ov} \times {\rm Min}\,(H_{\rm P}, r_{\rm co})\,, \quad (4)$$

where $\alpha_{\rm ov}$ is a free parameter and $r_{\rm co}$ is the radius of the convective core.

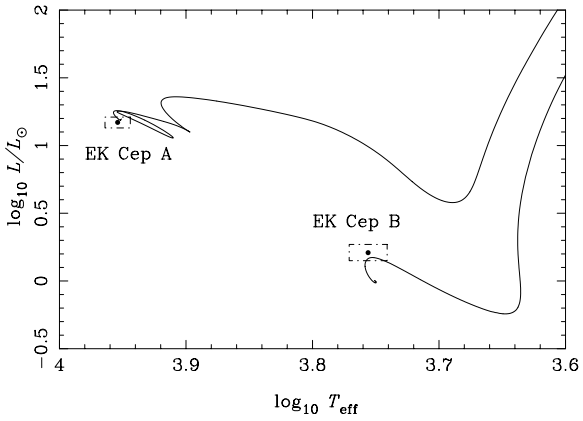

Fig. 7. Evolutionary tracks of EK Cep A and B on the HR diagram. These tracks were calculated including the effects of convective overshooting, with $\alpha_{\rm ov} = 0.20$.

Figure 7 shows evolutionary tracks calculated using $\alpha_{\rm ov} = 0.20$. The effects of the overshooting on the tracks are small for the track corresponding to EK Cep B; it merely extends the PMS phase, and makes the drop in luminosity near the end of the PMS phase more abrupt. This is caused by the fact that the central convective zone that appears at an age of about 25 Myr (see again Fig. 2) has a higher amount of ^{12}C to burn (the mixed zone extended by overshooting has a higher mass); the energy produced by ^{12}C-burning is higher, which causes the luminosity to drop more abruptly, and the fact that there is more ^{12}C to burn means that the ZAMS will arrive later (by about 10 Myr; the precise value depends on the parameter $\alpha_{\rm ov}$).

On the other hand, the track corresponding to EK Cep A is considerably changed with the inclusion of overshooting; it displays an extra "loop" after the first drop in luminosity (compare Figs. 3 and 7). This "loop" in the evolutionary track in the HR diagram is also seen (but not discussed) in the evolutionary tracks of Siess et al. (2000). It is caused by the following: as the ^{12}C in the central convective zone is been burned, its abundance drops and so does the rate of burning. As can be seen in Fig. 2, the central convective zone recedes towards the centre, leaving behind a zone of partially depleted ^{12}C. When the burning of ^{14}N becomes more efficient due to the rising central temperature, the convective zone expands again, englobing in the mixed central zone the unburned ^{12}C at the external regions. Now, as will be discussed in a subsequent

paper (Marques et al. in preparation), the extent of the mixed zone due to overshooting leaves more ^{12}C unburned in these regions; when this second expansion of the convective zone engulfs fresh ^{12}C, it does so at a rate faster than the burning time. The rising of the abundance of ^{12}C in the central convective region (which has now a much higher temperature than it had in the previous ^{12}C-burning phase) causes a large increase in the energy production through nuclear reactions in the core, which in turn makes the central convective region increase very rapidly, with the consequent rapid drop in the luminosity of the star. This extra "loop" in the evolutionary track in the HR diagram takes some 1.5 Myr; thus, the arrival on the ZAMS is delayed by a significant amount (for $\alpha_{\rm ov} = 0.2$, about 2.2 Myr).

For the present work, all these effects are of little importance. The age of the system EK Cep is greater than the age at which these effects take place for a star with the mass of EK Cep A, while it is lower than that at which overshooting starts to make a (small) difference for stars like EK Cep B. Our calibration is not, therefore, changed by the inclusion of convective overshooting. An alternative for studying the presence of overshooting in this system is the use of asteroseismology (e.g., Monteiro et al. 2000).

8. Conclusions

EK Cep is an excellent candidate to test stellar evolutionary models because it has one member in the MS phase and the other in the PMS phase. This difference in the evolutionary phase of the components results in a better calibration of the binary age of 26.8 Myr.

We have shown that an incorrect treatment of the time step for the evolution yields models with a lower luminosity during the PMS phase. If both stars are in the PMS phase, a large time step can be compensated for by a higher initial helium abundance (to increase the luminosity of the models; see Fig. 1). This cannot be done if the stars are in different evolutionary phases because the increase in the initial helium abundance will make both stars brighter, while only the PMS component has a lower luminosity, due to the larger time step. The dependence of the calibration on this key aspect of the modelling might explain the results obtained by Claret et al. (1995) and other results cited in Martín & Rebolo (1993), in particular that the radius (and luminosity) of EK Cep B are underestimated by evolutionary models. However, we cannot reproduce the radius of EK Cep A with our models. The presence of a fast rotating core (as in Yıldız 2003) would improve the situation. The use of a correct time step solves only part of the problem, by increasing the radius of EK Cep B and reducing the need for a larger radius of EK Cep A. We stress that our models were calculated using the metallicities obtained by Martín & Rebolo (1993); if a new determination of the metallicity is made, it would be possible to discern more clearly the origin of this inconsistency.

In the light of the new calibration, it becomes clear that EK Cep is an excellent binary to test different aspects of the physical processes of the evolution. Given the particular configuration of this system, one component (the primary) is insensitive to the mixing length parameter and age, while providing a very precise constraint on the helium abundance for the system. The effect of the overshooting on the evolutionary tracks of EK Cep A, although not relevant for this work, is important near the end of the PMS phase. We will explore the effects of the overshooting during the PMS evolution for various types of stars in a subsequent paper (Marques et al., in preparation). EK Cep B, still in the PMS, provides a very accurate indication of the age of the system, while being independent of the overshooting prescription. Such a combination makes EK Cep a test case of how the detailed observation of young binaries is of great relevance for improving the modelling of the evolution in this phase.

Acknowledgements. This work was supported in part by the *Fundação para a Ciência e a Tecnologia* through project POCTI/FNU/43658/2001. JPM was supported by grant SFRH/BD/9228/2002 from *Fundação para a Ciência e Tecnologia*. This work has been performed using the computing facilities provided by the CESAM stellar evolution code available at `http://www.obs-nice.fr/cesam/`
We thank the referee, F. Palla, for the many suggestions that improved so much the article.

References

Alexander, D. R., & Fergusson, J. W. 1994, ApJ, 437, 879
Andersen, J. 1991, A&AR, 3, 91
Angulo, C., Arnould, M., & the NACRE collaboration 1999, Nucl. Phys. A, 656, 3, and web site: `http://pntpm.ulb. ac.be/Nacre/nacre.htm`
Böhm-Vitense, E. 1958, ZAp, 54, 114
Claret, A., Giménez, A., & Martín, E. L. 1995, A&A, 302, 741
D'Antona, F., & Montalbán, J. 2003, A&A, 412, 213
Ebbighausen, E. G. 1966, AJ, 71, 642
Hill, G., & Ebbighausen, E. G. 1984, AJ, 89, 1256
Iben, I. 1965, ApJ, 141, 993
Iglesias, C. A., & Rogers, F. J. 1996, ApJ, 464, 943
Kippenhahn, R., & Weigert, A. 1991, Stellar Structure and Evolution (Springer-Verlag)
Lastennet, E., Valls-Gabaud, D., Lejeune, Th., & Oblak, E. 1999, A&A, 349, 485
Lastennet, E., Fernandes, J., Valls-Gabaud, D., & Oblak, E. 2003, A&A, 409, 611
Lee, C. W., Martín, E. L., & Mathieu, R. D. 1994, AJ, 108, 1445
Martín, E. L., & Rebolo, R. 1993, A&A, 274, 274
Monteiro, M. J. P. F. G., Christensen-Dalsgaard, J., & Thompson, M. J. 2000, MNRAS, 316, 165
Morel, P. 1997, A&AS, 124, 597
Morel, P., Morel, Ch., Provost, J., & Berthomieu, G. 2000a, A&A, 354, 636
Morel, P., Provost, J., Lebreton, Y., Thévenin, F., & Berthomieu, G. 2000b, A&A, 363, 675
Noels, A., Grevesse, N., Magain, P., et al. 1991, A&A, 247, 91
Palla, F., & Stahler, S. W. 1991, ApJ, 375, 288
Palla, F., & Stahler, S. W. 1992, ApJ, 392, 667
Palla, F., & Stahler, S. W. 2001, ApJ, 553, 299
Popper, D. M. 1987, ApJ, 313, L81
Rogers, F. J., Swenson, F. J., & Iglesias, C. A. 1996, ApJ, 456, 902
Siess, L., Dufour, E., & Forestini, M. 2000, A&A, 358, 593
Stahler, S. W. 1983, ApJ, 274, 822
Tomkin, J. 1983, ApJ, 271, 717
Yıldız, M. 2003, A&A, 409, 689